

Meson-Dominance Implications for the Bottomness-Preserving Decays of the B_c Meson*

P. Lichard

Institute of Physics and Centre for Computational Physics and Data Processing,
Silesian University in Opava, 746 01 Opava, Czech Republic and Institute of Experimental and
Applied Physics, Czech Technical University in Prague, 128 00 Prague, Czech Republic

We present the meson-dominance predictions for the bottomness-preserving branching fractions of the B_c meson normalized to the $B_c \rightarrow B_s^0$ decay mode. To give a credibility to our predictions, we first test our model in the case of the $B \rightarrow \bar{D}^0$ transitions, where the branching ratios are experimentally known. Comparison with the previous results based on different approaches is given.

In 2013, the LHCb collaboration at the CERN LHC collider announced [1] the observation of the $B_c \rightarrow B_s^0$ decay mode with significance in excess of five standard deviations. Even now, after the Run 2 of the LHC collider stretching from 2015 to 2018, this mode remains the only experimentally confirmed bottomness-preserving (BP) decay mode of the B_c meson.

In this note we present the estimates of the branching ratios of other BP decays of the B_c relative to the already observed one. We use the meson dominance (MD) model [2], which describes well the meson decays that fall into the “external W-emission” category according to the quark-diagram nomenclature [3]. To assess the credibility of our predictions for the B_c branching ratios, we first calculate similar branching ratios connected with the $B \rightarrow \bar{D}^0$ transition and compare them to data.

The decay of a positive pseudoscalar (PS) meson P_1 (B or B_c) into a neutral PS meson P_2 (\bar{D}^0 , B_s^0 or B^0) and a positive PS meson P_3 (π or K) is described by a diagram depicted in Fig. 1. The diagram contains a strong interaction vertex entered by P_1 , P_2 , and a positive vector meson V with flavor quantum numbers required by the conservation laws. The vector meson then couples to the gauge boson W , which in turn couples to the outgoing pseudoscalar meson P_3 . The corresponding partial decay width is given by Eq. (4.8) from [2], which we reproduce for the reader’s convenience here.

$$\Gamma(P_1 \rightarrow P_2 P_3) = \frac{G_F^2 X_{P_1 P_2 V} Z_{P_3}}{16 m_1^3} (m_1^2 - m_2^2)^2 \sqrt{(m_1^2 - m_2^2)(m_1^2 - m_3^2)(m_2^2 - m_3^2)}. \quad (1)$$

Function X is defined by $X = x^2 + y^2 + z^2 - 2xy - 2xz - 2yz$. The dimensionless parameter

$$X_{P_1 P_2 V} = \left| w_V V_V \frac{g_{VP_1 P_2}}{g} \right|^2$$

*Dedicated to Professor Peter Prešnajder on the occasion of his 70th birthday

includes the strong coupling constant $g_{VP_1P_2}$, the coupling constant g , the element V_V of the CKM matrix pertinent to valence quark and antiquark of the meson V , and a dimensionless parameter $w_V = 1$ characterizing the deviation of the $V-W$ coupling from the W one. At present, there is no chance of getting the value of X_{B_c, B_s^0, D_s^*} from its components. This unknown quantity cancels in the branching ratios we calculate in this work.

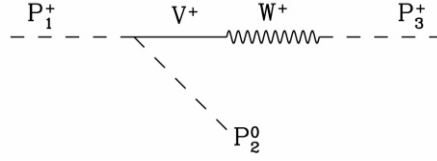


Fig. 1. Decay $P_1^+ \rightarrow P_2^0$ in the MD model.

The parameter Z_P , which is another important ingredient of Eq. (1), is defined in terms of the pseudoscalar decay constant f_P and the CKM matrix element V_P corresponding to the valence quark composition of a particular pseudoscalar meson P by

$$Z_P = |f_P V_P|^2. \quad (2)$$

Its value is determined from the muonic decay width given by the formula [2]

$$\Gamma(P \rightarrow \mu^+ \nu_\mu) = \frac{G_F^2}{2} Z_P m_\mu^2 \left(1 - \frac{m_\mu^2}{m_P^2}\right)^2 \mathcal{O}(\alpha_s).$$

We have included the radiative corrections $\mathcal{O}(\alpha_s)$ following [4]. The results obtained by using the experimental muonic decay widths [5] are shown in Table I. It follows from Eq. (1) that the branching ratio between the K and P modes is given by

$$\frac{\mathcal{B}(P_1^+ \rightarrow P_2^0 K^+)}{\mathcal{B}(P_1^+ \rightarrow P_2^0 P^+)} = \frac{Z_K}{Z_P} \sqrt{\frac{(m_1^2, m_2^2, m_K^2)}{(m_1^2, m_2^2, m^2)}}. \quad (3)$$

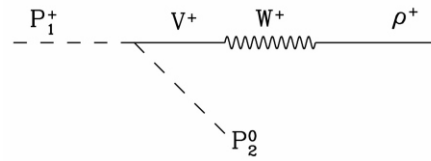


Fig. 2. Decay $P_1^+ \rightarrow P_2^0$ in the MD model.

Table I. Parameters Z_P characterizing the coupling of pseudoscalar mesons to the charged gauge boson and their sources. For definition, see Eq. (2).

P	$Z_P (\text{MeV}^2)$	Source
	$(1.6158 \pm 0.0019) \cdot 10^4$	
K	$(1.2307 \pm 0.0032) \cdot 10^3$	K

We will also consider decay mode with the vector meson in the final state, depicted in Fig. 2. Its decay width is given by Eq. (4.9) in [2]. After substituting $|V_{ud}|^2$ for Y there (see Table I in [2]), we obtain

$$\Gamma(P_1 \rightarrow P_2) = \frac{G_F^2 m^2 X_{P_1 P_2 V} |V_{ud}|^2}{8 g^2 m_1^3} \frac{m_V^2}{m_V^2 - m^2} {}^{3/2}(m_1^2, m_2^2, m^2).$$

After dividing this decay width by that given in Eq. (1), we eliminate the unknown factor $X_{P_1 P_2 V}$ and obtain the branching ratio formula

$$\frac{\Gamma(P_1 \rightarrow P_2)}{\Gamma(P_1 \rightarrow P_2)} = \frac{2m^2 |V_{ud}|^2}{g^2 Z (m_1^2 - m_2^2)^2} \frac{{}^{3/2}(m_1^2, m_2^2, m^2)}{{}^{1/2}(m_1^2, m_2^2, m^2)} \frac{m_V^2}{m_V^2 - m^2}. \quad (4)$$

We use $|V_{ud}| = 0.97420$ [5] and $g^2 = 35.72$. The latter value follows from the formula

$$\frac{g^2}{48 m^2} (m^2 - 4m^2)^{3/2}$$

and the central values of the parameters $m = 775.26$ MeV and $m_V = 149.1$ MeV [5].

The semileptonic decay $P_1 \rightarrow P_2 \ell \bar{\ell}$ in the MD model is described by the diagram in Fig. 3. The differential decay width in t , which is the square of the four-momentum transfer from P_1 to P_2 , is given by

$$\frac{d\Gamma(P_1 \rightarrow P_2 \ell \bar{\ell})}{dt} = \frac{G_F^2 X_{P_1 P_2 V} m_V^2}{9 m_1^3} \frac{m_V^2}{m_V^2 - t} {}^{3/2}(m_1^2, m_2^2, t). \quad (5)$$

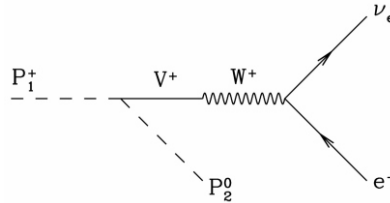


Fig. 3. The semileptonic decay of the P_1 to P_2 meson in the MD model.

Formula (5) is a simplified version of Eq. (4.3) in Ref. [2] obtained by assuming that the lepton mass is negligible. After dividing Eq. (5) by Eq. (1), the unknown X -factor cancels again and we obtain

$$\frac{d\Gamma(P_1 \rightarrow P_2 \ell \bar{\ell})}{dt} = \frac{m_V^4}{6^2 Z (m_1^2 - m_2^2)} {}^{1/2}(m_1^2, m_2^2, m^2) \int_0^{t_M} \frac{{}^{3/2}(m_1^2, m_2^2, t)}{(m_V^2 - t)^2} dt, \quad (6)$$

where $t_M = (m_1 - m_2)^2$.

We first apply our model to the transition $B \rightarrow \bar{D}^0$, for which the branching fractions to the final states with K , π , and $\ell \bar{\ell}$ have been measured. We calculate the branching ratios by means of formulas (3), (4), and (6), in which we replace P_1 by B and P_2 by \bar{D}^0 . Flavor conservation requires that the place of the intermediate vector meson V be taken by B_c^* , which has not been observed yet. We use for its mass a value of $6.34 \text{ GeV}/c^2$, determined by Godfrey and Isgur [6] in a relativized quark model with

chromodynamics. This value agrees [7] with results of other potential models and from lattice quantum chromodynamics calculations.

The results of our calculations are shown in Table II together with branching ratios evaluated from the experimental branching fractions $\mathcal{B}(B \rightarrow \bar{D}^0) = (4.68 \pm 0.13) \times 10^{-3}$, $\mathcal{B}(B \rightarrow \bar{D}^0 K) = (3.63 \pm 0.12) \times 10^{-4}$, $\mathcal{B}(B \rightarrow \bar{D}^0 \ell) = (1.34 \pm 0.18) \times 10^{-2}$, and $\mathcal{B}(B \rightarrow \bar{D}^0 \ell \ell) = (2.20 \pm 0.10) \times 10^{-2}$ [5]. The relative errors of the resulting branching ratios were calculated as a sum of relative errors of the individual branching fractions.

Table II. Branching ratios between various $B \rightarrow \bar{D}^0$ transitions.

Branching ratio	MD model	Experiment [5]
$\bar{D}^0 K / \bar{D}^0$	$7.53 \cdot 10^{-2}$	$(7.76 \cdot 10^{-2})$
$\bar{D}^0 \ell \ell / \bar{D}^0$	5.2	4.70 0.34
\bar{D}^0 / \bar{D}^0	$(1.85) \cdot 2.7^a$	2.86 0.46

^a After the correction described in the text.

Of the three calculated B branching ratios, the first two, namely $\bar{D}^0 K / \bar{D}^0$ and $\bar{D}^0 \ell \ell / \bar{D}^0$, agree with data well. For the \bar{D}^0 / \bar{D}^0 ratio we get from Eq. (4) a value of 1.85, which is about 1.5 times smaller than the experimental value. It is interesting that a similar factor appears in the dielectron decay of the neutral meson. When we use the vector-meson dominance (VMD) to calculate the dielectron decay width assuming that the coupling constant in the W junction is equal to that fixed by the normalization of the pion form factor, namely $g_{\rho} = em^2 / g$, we get

$$\left(\bar{D}^0 \rightarrow e e \right)_{VMD} = \frac{2(m^2 - 4m^2)^{3/2}}{36m} (4.845 \cdot 0.031)$$

where α is the fine-structure constant. The ρ -resonance parameters were taken from [5] and the errors originating in m and α were summed linearly. Comparison with the experimental decay width of (7.04 ± 0.06) keV [5] leads to

$$\frac{\left(\bar{D}^0 \rightarrow e e \right)_{\text{exp.}}}{\left(\bar{D}^0 \rightarrow e e \right)_{VMD}} = 1.453 \cdot 0.022. \quad (7)$$

One possible explanation of the $\bar{D}^0 \rightarrow e e$ conundrum is that the \bar{D}^0 coupling constant is q^2 -dependent with $g_{\rho}^2(m^2)$ larger than $g_{\rho}^2(0)$ by a factor given by Eq. (7).

To remove the discrepancy of the $\mathcal{B}(B \rightarrow \bar{D}^0) / \mathcal{B}(B \rightarrow \bar{D}^0 K)$ ratio with experiment, we will assume that the coupling constant in the W junction g_w is q^2 -dependent in the same way as the g_{ρ} . We thus get the corrected branching ratio of $1.85 \cdot 1.453 \cdot 2.7$, in agreement with experiment, see Table II.

After having checked the soundness of the MD approach, we turn to the predictions of the branching ratios connected with the $B_c \rightarrow B_s^0$ and $B_c \rightarrow B^0$ transitions. We again use Eqs. (3), (4), and (6). First we replace P_1 by B_c , P_2 by B_s^0 , and V by D_s^* . The prediction of the MD model for the $B_c \rightarrow B_s^0 K$, $B_c \rightarrow B_s^0 e e$, and $B_c \rightarrow B_s^0$ branching fractions relative to the $B_c \rightarrow B_s^0$ branching fraction are shown in the first three rows of Table III together with the results of other works. In the case of the B_s^0 final state we quote two

values: uncorrected (in parentheses) and corrected by including the factor of 1.453 inspired by Eq. (7).

The analogous results for the $B_c \rightarrow B$ transitions, which are obtained when P_2 is set to B and $V \rightarrow D^*$, are listed in rows 4–6 of Table III.

We can also compare the branching fractions of the modes with different B -mesons in the final states, e.g.,

$$\frac{\mathcal{B}(B_c \rightarrow B^0)}{\mathcal{B}(B_c \rightarrow B_s^0)} = R_X \frac{m_{B_c}^2}{m_{B_c}^2} \frac{m_{B^0}^2}{m_{B_s^0}^2} \sqrt{\frac{(m_{B_c}^2, m_{B^0}^2, m^2)}{(m_{B_c}^2, m_{B_s^0}^2, m^2)}},$$

where

$$R_X = \frac{X_{B_c B^0 D^*}}{X_{B_c B_s^0 D^*}}$$

is an unknown quantity. We can get a crude estimate of its value if assuming that the light-flavor SU(3) symmetry is only mildly broken. Then we can write

$$R_X \left| \frac{V_{cd}}{V_{cs}} \right|^2 = 5.3 \cdot 10^{-2}$$

and

$$\frac{\mathcal{B}(B_c \rightarrow B^0)}{\mathcal{B}(B_c \rightarrow B_s^0)} = 7 \cdot 10^{-2}.$$

This estimate is compared to the results of other authors in the last row of Table III.

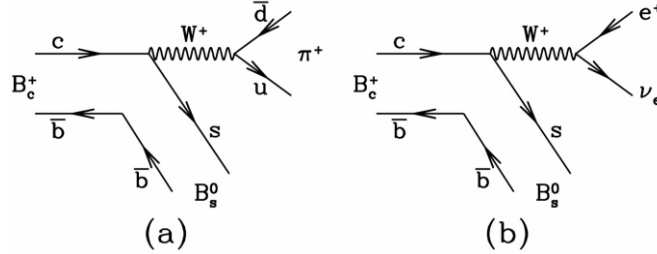


Fig. 4. Quark-line diagrams of decays: (a) $B_c \rightarrow B^0 \pi^+$ and (b) $B_c \rightarrow B^0 e^+ \nu_e$.

It has been shown in several theoretical studies, see, e.g., Refs. [16, 17], that the rates of decay modes to the excited vector states of the B_s^0 and B^0 are almost as intensive as the transition rates to the ground states. Unfortunately, we cannot address this issue in the MD model yet. The $P \rightarrow V$ transitions require an axialvector meson in the intermediate state. And the strong PVA coupling is more difficult to describe than the PPV coupling, which we explore in this work. In addition, also the intermediate states with pseudoscalar mesons can contribute, what would make the MD predictions of the transitions from B_c to B_s^{*0} or B^{*0} even vaguer.

Our results on the B_c branching ratios, presented in Table III fall in the range defined by the results of previous works. For the ratios related to the π -meson it is true only after the VMD-inspired correction.

The application of the MD model to the bottomness-preserving CKM-allowed two-meson decays of the B_c meson is possible thanks to the fact that they belong to the class of the external W -exchange diagrams according to the quark phenomenology nomenclature [3]. The structure of those diagrams is the same as that of the semileptonic decays, see an example in Fig. 4. If the contribution from diagrams of other classes is none or negligible, the MD provides a good description of branching ratios, see [2] and Table II here. In exceptional cases, with the charged B_c -meson (the coupling of which to the W -boson is fixed by the normalization condition [2]) in the intermediate state, e.g., $B_c^0 \rightarrow e^+ e^-$, it yields the partial decay width. The basic assumption of the MD approach is that the QCD corrections generate an intermediate meson state, so we can take them into account by working directly with that meson, as shown in Figs. 1, 2, and 3.

Table III. Branching ratios between various bottomness-preserving decay modes of the B_c meson. The numbers in square brackets denote the references to previous works.

Branching ratio	This work	[8]	[9]	[10]	[11]	[12]	[13]	[14]	[15]	[16, 17]
$B_c^0 K / B_c^0$	0.065	0.072	0.070	0.11		0.065	0.083	0.074		0.066
B_c^0 / B_c^0	(0.38) 0.56 ^a	0.77	0.44	2.5	0.42	0.44	0.56	0.59	1.5	0.83
$B_c^0 e^- / B_c^0$	0.39	0.36	0.20	0.50 ^b	0.23	0.25	0.33	0.28		0.32 (0.35) ^c
$B_c^0 K / B^0$	0.067	0.077	0.071	0.10		0.066	0.090	0.075		0.071
B^0 / B^0	(0.66) 0.97 ^a	1.81	0.78	2.73		0.91	1.30	1.00		1.64
$B^0 e^- / B^0$	0.46	0.56	0.25	0.61 ^b		0.32	0.42	0.35		0.42 (0.45) ^c
B^0 / B_s^0	0.07	0.056	0.064	0.065		0.065	0.040	0.051		0.066

^aAfter the correction described in the text.

^bUsing $a_1^c = 1.351$ [9] to get $(B_c \rightarrow \{B_s^0\} B^0)$.

^cUsing $a_1^c = 1.24$ (1.2) [17] to get $(B_c \rightarrow \{B_s^0\} B^0)$.

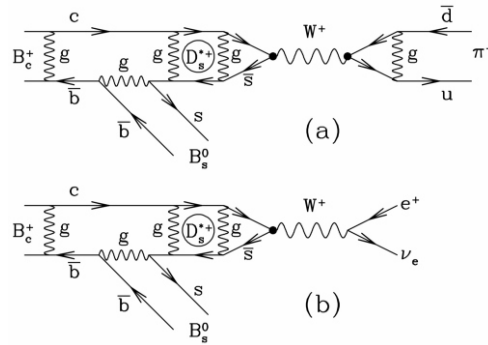


Fig. 5. Quark-line diagrams with several gluon lines symbolizing the QCD corrections: (a) $B_c \rightarrow B_s^0$ (b) $B_c \rightarrow B_s^0 e^- e^-$.

There is a special feature which distinguishes the MD model from other approaches listed in Table III. Because of the identical structure of the quark system which couples to the W -boson, see Fig. 4, the semileptonic decay modes acquire the same QCD corrections as the hadronic modes that belong to the external W -emission category. This is visualized in Fig. 5. The QCD correction factor does not depend on the system that is produced in the final state by the W conversion. The branching ratios of a semileptonic to hadronic modes is thus not influenced by the QCD corrections. This is not true in other approaches, which require knowledge of a QCD factor related to the Wilson coefficients when determining such branching ratios.

What concerns the prospects of discovering yet unknown bottomness-preserving decay modes of the B_c meson, one cannot expect any contribution from the experiments at the e^+e^- colliders because they operate at energies below the threshold for B_c production. So only hadron collider experiments are currently able to study the B_c sector. Some results may come from the CDF and D0 experiments, which are still analyzing the data sets collected at the Tevatron collider until 2011. The LHC Run 2 ended on December 3, 2018 and a flow of results from the LHC experiments will start again in 2021. Of them, the LHCb, the first dedicated beauty experiment at the hadron collider, will again be in the best position to study the B_c decays. During the forthcoming two year-long LHC shutdown the current experiment will be largely dismantled and an almost completely new detector will be constructed. The major fraction of LHCb's sub-detectors will be replaced or upgraded [18].

I am indebted to Dr. Tim Gershon for useful correspondence. This work was partly supported by the Ministry of Education, Youth and Sports of the Czech Republic Inter-Excellence project No. LTI17018.

References

- [1] R. Aaij et al.: (LHCb Collaboration), Phys. Rev. Lett. **111** (2013) 181801.
- [2] P. Lichard: Phys. Rev. D **55** (1997) 5385.
- [3] L.-L. Chau: Phys. Rep. **95** (1983) 1.
- [4] V. Cirigliano and I. Rosell: JHEP**10** (2007) 5.
- [5] M. Tanabashi et al.: (Particle Data Group), Phys. Rev. D **98** (2018) 030001.
- [6] S. Godfrey and N. Isgur: Phys. Rev. D **32** (1985) 189.
- [7] S. Godfrey: Phys. Rev. D **70** (2004) 054017, and references therein.
- [8] C.-H. Chang and Y.-Q. Chen: Phys. Rev. D **49** (1994) 3399.
- [9] P. Colangelo and F. De Fazio: Phys. Rev. D **61** (2000) 034012.
- [10] A. Abd El-Hady, J. H. Muñoz, and J. P. Vary: Phys. Rev. D **62** (2000) 014019.
- [11] V. V. Kiselev, A. E. Kovalsky, and A. K. Likhoded: Nucl. Phys. B **585** (2000) 353.
- [12] I. Gouz, V. V. Kiselev, A. K. Likhoded, V. I. Romanovsky, and O. P. Yushchenko: Yad. Fiz. **67** (2004) 1581 [Phys. At. Nucl. **67** (2004) 1559].
- [13] D. Ebert, R. N.Faustov, and V. O. Galkin: Eur. Phys. J. C **32** (2003) 29.
- [14] M. A. Ivanov, J. G. Körner, and P. Santorelli: Phys. Rev. D **73** (2006) 054024.
- [15] R. Dhir, N. Sharma, and R. C. Verma: J. Phys. G **35** (2008) 085002;
R. Dhir and R. C. Verma: Phys. Rev. D **79** (2009) 034004.
- [16] N. Barik, S. Naimuddin, P. C. Dash, and S. Kar: Phys. Rev. D **80** (2009) 074005.
- [17] S. Naimuddin, S. Kar, M. Priyadarsini, N. Barik, and P. C. Dash: Phys. Rev. D **86** (2012) 094028.
- [18] <http://lhcb-public.web.cern.ch/lhcb-public/>

